Proc. Natl. Acad. Sci. USA
Vol. 91, pp. 8890–8894, September 1994
Neurobiology

Heteromeric olfactory cyclic nucleotide-gated channels: A subunit that confers increased sensitivity to cAMP

(olfaction/cGMP)

JONATHAN BRADLEY, JUN LI, NORMAN DAVIDSON, HENRY A. LESTER, AND KAI ZINN*

Division of Biology, California Institute of Technology, Pasadena, CA 91125

Contributed by Norman Davidson, May 20, 1994

ABSTRACT **Olfactory receptor neurons respond to odorant stimulation with a rapid increase in intracellular cAMP that opens cyclic nucleotide-gated (cng) cation channels. cng channels in rat olfactory neurons are activated by cAMP in the low micromolar range and are outwardly rectifying. The cloned rat olfactory cng channel (rOCNC1), however, is much less sensitive to cAMP and exhibits very weak rectification. Here we describe the cloning and characterization of a second rat cng channel subunit, denoted rOCNC2. rOCNC2 does not form functional channels when expressed alone. When rOCNC1 and rOCNC2 are coexpressed, however, an outwardly rectifying cation conductance with cAMP sensitivity near that of the native channel is observed. *In situ* hybridization with probes specific for the two subunits shows that they are coexpressed in olfactory receptor neurons. These data indicate that the native olfactory cng channel is likely to be a heterooligomer of the rOCNC1 and rOCNC2 subunits.**

One mechanism of olfactory signal transduction involves a rapid and transient increase in intracellular cAMP. In response to the binding of odorants, guanine nucleotide-binding protein (G protein)-coupled receptors activate a G_s-like G protein which increases the enzymatic activity of adenylyl cyclase (reviewed in refs. 1 and 2). The resulting increase in cAMP opens cyclic nucleotide-gated (cng) cation channels in the cilia and dendrites of olfactory receptor neurons. This produces an influx of monovalent and divalent cations, depolarizing the neurons (3–7). The influx of Ca^{2+} activates an outward Cl^- conductance (8–10), and Cl^- efflux acts to amplify the initial depolarization, triggering sensory nerve impulses.

Molecular data support this model of olfactory signal transduction. Olfactory receptor neurons express a very large family of G protein-coupled receptors (11). These receptors could interact with G_{olf}, a G protein also expressed in olfactory neurons that is very similar in sequence to G_s (12). An adenylyl cyclase (13) and a cng channel (14–16) have also been cloned from olfactory epithelium and characterized.

The rat olfactory cng channel clone rOCNC1 forms cAMP-activated channels when heterologously expressed in mammalian cells. The conductance is characterized by a half-maximally effective concentration (EC_{50}) for cAMP of 68 μM and very weak rectification in the absence of divalent cations (14). In contrast, the native conductance in rat olfactory neurons is much more sensitive to cAMP (EC_{50} of 2.5 μM) and is outwardly rectifying (7). There are several possible explanations for these functional differences. For example, a second olfactory channel might exist that would display the cAMP sensitivity and rectification behavior of the native channel when heterologously expressed. Alternatively, another channel subunit might modulate the properties of rOCNC1 by forming heterooligomeric channels with it.†

MATERIALS AND METHODS

rOCNC2 cDNA Clones. Primers CN2 [5′-AARYTIGCIG-TIGTNGCNGA-3′, corresponding to rOCNC1 aa 500–506 (Lys-Leu-Ala-Val-Val-Ala-Asp)] and CN1 [5′-AT(R)TTI-GCIGTIC(K)IC(K)(R)TTNCC, corresponding to aa 535–542 (Gly-Asn-Arg-Arg-Thr-Ala-Asn-Ile)] were used for polymerase chain reaction (PCR) (17) experiments using oligo(dT)-primed first-strand cDNA synthesized from template rat nasal epithelial RNA. The annealing temperature was 42°C and 35 amplification cycles were performed. Restriction analysis of the PCR product revealed that it contained two sequence classes; one of these corresponded to the rOCNC2 sequence. To obtain an rOCNC2-specific hybridization probe, an rOCNC2-specific PCR primer was designed from aa 417–426 and used in combination with vector primers flanking the polylinker of λZAPII (Stratagene) to PCR amplify sequences from a rat nasal epithelial λZAPII cDNA library. The ends of the 1090-bp fragment thus isolated were sequenced, and new rOCNC2-specific PCR primers were designed and used to amplify a non-cross-hybridizing fragment of 820 bp. This was used to screen 1.8×10^6 phage from the library and 8 full-length rOCNC2 clones were isolated; 2 of these were sequenced (29). We sequenced the 5′ ends of all 8 clones to determine whether a second form of rOCNC2 with a longer N terminus might exist, but we found no evidence for such a form.

Channel mRNA Levels. cDNA was quantitated by amplifying with β-actin primers (15 and 20 cycles) and the amounts of cDNA in each channel primer amplification were adjusted on the basis of these results. Primer sequences are available on request. For the channel mRNA amplifications ≈1 ng of cDNA was amplified for 25, 30, or 35 cycles. The amplification products were electrophoresed in a 1.5% agarose gel, stained with ethidium bromide, and photographed.

***In Situ* Hybridization.** Digoxigenin antisense RNA probes were synthesized with an *in vitro* transcription kit (Ambion, Austin, TX) in the presence of digoxigenin-UTP (at a ratio of 1:3 relative to UTP). The G_{olf} probe template was a full-length cDNA clone of 3 kb. The I7 receptor probe template was the entire coding sequence (984 bp). rOCNC1 and rOCNC2 probe templates were generated from pBluescript (Stratagene) clones of rOCNC1 and rOCNC2 by PCR using primers 1849 (rOCNC1; corresponding to aa 624–630) and 1666 (rOCNC2; aa 518–524), in combination with vector primers flanking the transcription promoters at the 3′ ends of these

The publication costs of this article were defrayed in part by page charge payment. This article must therefore be hereby marked "*advertisement*" in accordance with 18 U.S.C. §1734 solely to indicate this fact.

Abbreviations: cng, cyclic nucleotide-gated; CN, cyclic nucleotide-binding domain; HEK, human embryonic kidney; V_m, membrane potential.

*To whom reprint requests should be addressed.

†The sequence reported in this paper has been deposited in the GenBank data base (accession no. U12623).

```
rOCNC1   MMTEKSNGVK SSPANNENHH PPPSIKANGK DDERAGSRPQ SVAADDDTSP   50
rOCNC1   ELQRLAEMDT PRRGRGGFQR IVRLVGVIRD WANKNFREEE PRPDSFLERF  100

rOCNC2         MS QDGKVKTTES TPPAPTKARK WLPVLDPSGD YYYWWLNTMV   42
rOCNC1   RGPELQTVTT HQGDDKGGKD GEGKGTKKKF ELFVLDPAGD WYYRWLFVIA  150
Consensus ......... ..G..K.... .....TK... .L.VLDP.GD .YY.WL....  150
                S1                    S2
rOCNC2   FPIMYNLIIV VCRACFPDLQ HSYLVAWFVL DYFSDLLYLL DIGVRFHTGF   92
rOCNC1   MPVLYNWCLL VARACFSDLQ RNYFVVWLVL DYFSDTVYIA DLIIRLRTGF  200
Consensus .P..YN.... V.RACF.DLQ ..Y.V.W.VL DY.SD..Y.. D...R..TGF  200
                                S3
rOCNC2   LEQGILVVDK GMIASRYVRT WSFLLDLASL VPTDAAYVQL GFHIPTLRLN  142
rOCNC1   LEQGLLVKDP KKLRDNYIHT LQFKLDVASI IPTDLIYFAV GIHSPEVRFN  250
Consensus LEQG.LV.D. ......Y..T ..F.LD.AS. .PTD..Y... G.H.P..R.N  250
              S4                        S5
rOCNC2   RFLRVPRLFE AFDRTETRTA YPNAFRIAKL MLYIFVVIHW NSCLYFALSR  192
rOCNC1   RLLEFARMFE FFDRTETRTS YPNIFRISNL VLYILVIIHW NACIYYVISK  300
Consensus R.L...R.FE .FDRTETRT. YPN.FRI..L .LYI.V.IHW N.C.Y...S.  300
                                    P
rOCNC2   YLGFGRDAWV YPDPAQPGFE RLRRQYLYSF YFSTLILTTV GDTPLPDREE  242
rOCNC1   SIGFGVDTWV YPNITDPEYG YLAREYIYCL YWSTLTLTTI GETPPPVKDE  350
Consensus ..GFG.D.WV YP....P... .L.R.Y.Y.. Y.STL.LTT. G.TP.P...E  350
                S6
rOCNC2   EYLFMVGDFL LAVMGFATIM GSMSSVIYNM NTADAAFYPD HALVKKYMKL  292
rOCNC1   EYLFVIFDFL IGVLIFATIV GMVGSMISNM NATRAEFQAK IDAVKHYMQF  400
Consensus EYLF...DFL ..V..FATI. G...S.I.NM N...A.F... ...VK.YM..  400

rOCNC2   QHVNKRLERR VIDWYQRLQI NKKMTNEVAI LQHLPERLRA EVAVSVHLST  342
rOCNC1   RKVSKDMEAK VIKWFDYLWT NKKTVDEREV LKNLPAKLRA EIAINVHLST  450
Consensus ..V.K..E.. VI.W...L.. NKK...E... L..LP..LRA E.A..VHLST  450
                          Cyclic Nucleotide Binding Domain
rOCNC2   LSRVQIFQNC EASLLKELVL KLQPQTYSPG EYVCREGDIG REMYIIREGQ  392
rOCNC1   LKKVRIFQDC EAGLLVELVL KLRPQVFSPG DYICREKGDIG KEMYIIKEGK  500
Consensus L..V.IFQ.C EA.LL.ELVL KL.PQ..SPG .Y.CREGDIG .EMYII.EG.  500

rOCNC2   LAVVADDGVT QYAVLGAGLY FGEISIINIK GMMSGNRRTA NIKSLGYSDL  442
rOCNC1   LAVVADDGVT QYALLSAGSC FGEISILNIK GSKMGNRRTA NIRSLGYSDL  550
Consensus LAVVADDGVT QYA.L.AG.. FGEISI.NIK G...GNRRTA NI.SLGYSDL  550

rOCNC2   FCLSKEDLRE VLSEYPQAQA VMEEEGREIL LKMNKLDVNA EAAEIALQEA  492
rOCNC1   FCLSKDDLME AVTEYPDAKK VLEERGREIL MKEGLLDENE VAASMEVD--  598
Consensus FCLSK.DL.E ...EYP.A.. V.EE.GREIL .K...LD.N. .AA.......  600

rOCNC2   TESRLKGLDQ QLDDLQTKFA RLLAELESSA LKIAYRIERL EWQTREWPMP  542
rOCNC1   VQEKLEQLET MMDTLYTRFA RLLAEYTGAQ QKLKQRITVL E--TK-----  641
Consensus ....L..L.. ..D.L.T.FA RLLAE..... .K...RI..L E..T.....  650

rOCNC2   EDMGEADDEA EPGEGTSKDG EGKAGQAGPS GIE                    575
rOCNC1   --MKQNHEDD YLSDGINT-- ------PEPT AAE                    664
Consensus ..M..... ....G..... ........P. ..E                    683
```

FIG. 1. Aligned amino acid sequences of rOCNC1 and rOCNC2 proteins. In the alignment, a dash indicates the absence of an amino acid, and a dot in the consensus line indicates an amino acid that is not conserved between the sequences. S1–S6 are putative transmembrane domains, and P is the putative pore region. The cyclic nucleotide-binding (CN) domain is defined by homology to the sequences of other proteins that bind cAMP and cGMP (20, 21).

genes. These probes did not cross-hybridize to the other channel sequence by Northern blot analysis using full-length sense-strand *in vitro* transcripts of rOCNC1 and rOCNC2 cDNA clones (J.B., unpublished results). *In situ* hybridization was performed as described (18). Sections were mounted in glycerol and photographed under coverslips with a Zeiss Axioplan microscope.

Electrophysiology. The pCIS expression vector was used and transfections into human embryonic kidney (HEK) 293 cells were performed as described (19). Patch-clamp recordings were made 1–3 days after transfection. Electrodes were fabricated from borosilicate glass and had resistances of 1–3 MΩ. Cyclic nucleotides were applied by a fast microperfusion system that allowed solution changes within 100 ms. Divalent cation-free solution was 140 mM NaCl/5 mM KCl/10 mM Na Hepes/0.5 mM Na EDTA/0.5 mM Na EGTA, pH 7.6. Solution with divalents was 140 mM NaCl/5 mM KCl/10 mM Na Hepes/2 mM $CaCl_2$/1 mM $MgCl_2$, pH 7.6. Single-channel recordings were made from excised inside-out patches with symmetrical divalent cation-free solutions. Data were filtered at 2 kHz, digitized at 16-bit resolution and 22-kHz frequency for storage on magnetic tape, and redigitized and analyzed at 4 kHz with AXOTAPE 2.0/FETCHAN 6.0 (Axon Instruments, Foster City, CA).

RESULTS

We used PCR to amplify cng channel-related sequences from primary olfactory epithelial cDNA. We identified an amplification product whose sequence is closely related to rOCNC1. This product was used to isolate a full-length cDNA clone, denoted rOCNC2. The predicted amino acid sequence of rOCNC2 comprises 575 residues and is 51% identical to rOCNC1 (Fig. 1). Hydropathy plots of the two sequences are almost superimposable, indicating similar transmembrane topology. Each protein contains six putative transmembrane regions (S1–S6), and a pore (P) region homologous to the P region of voltage-gated channels.

The CN domain is highly conserved (77% identity). A threonine residue which influences selectivity for cGMP over cAMP (22) is present in both sequences (residue 539 in rOCNC1). However, there are three adjacent nonconservative differences Ser-Lys-Met (aa 532–534) in rOCNC1 vs. Asn-Met-Ser (aa 424–426) in rOCNC2 within the most conserved part of the CN domain (20, 21). The S4 region of rOCNC2, which corresponds to the putative voltage sensor of voltage-gated channels, is likely to bear one or two more positive charges than the corresponding sequence from rOCNC1 (two if His^{254} of rOCNC1 is uncharged). The two sequences also differ at a position in the P region (Glu^{342} in rOCNC1, which corresponds positionally to Asp^{234} in rOCNC2) that influences interactions between divalent cat-

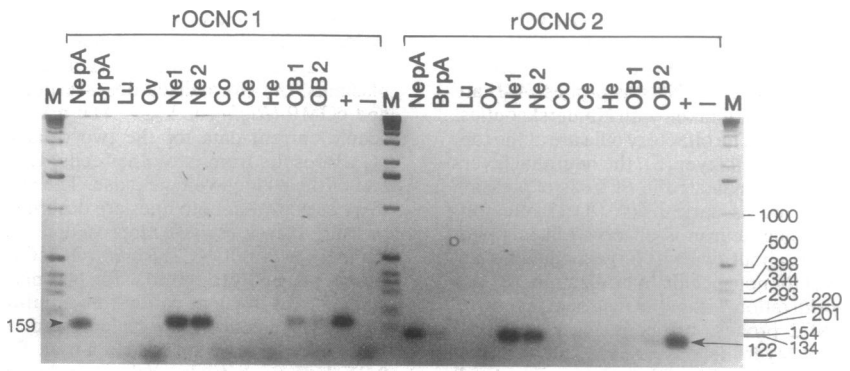

FIG. 2. Expression pattern of rOCNC1 (*Left*) and rOCNC2 (*Right*) mRNAs, as determined by quantitative reverse transcription–PCR. Primers specific for the 3′ untranslated regions of the two mRNAs were used to amplify oligo(dT)-primed cDNA made from RNA isolated from various rat tissues. Total RNA was used except where indicated. This is a negative image of the ethidium bromide-stained agarose gel. The rOCNC1 PCR product is 159 bp, and the rOCNC2 product is 122 bp. Lanes: M, markers (sizes in bases indicated at right); NepA, nasal epithelium [poly(A)$^+$ RNA]; BrpA, brain [excluding olfactory bulb; poly(A)$^+$ mRNA]; Lu, lung; Ov, ovary; Ne1 and Ne2, nasal epithelium (two isolates); Co, cortex; Ce, cerebellum; He, heart; OB1 and OB2, olfactory bulb (two isolates); +, positive control (rOCNC1 or rOCNC2 plasmid clone); −, negative control (no DNA).

ions and the channel pore (23–25). Finally, rOCNC2 is 109 aa shorter than rOCNC1 at its N terminus.

We used quantitative reverse transcription–PCR to assay the tissue-specific expression patterns of the rOCNC1 and rOCNC2 mRNAs. A 30-cycle amplification is shown in Fig. 2; both mRNAs are highly enriched in the olfactory epithelium, although low-level expression can be detected in brain and olfactory bulb. In 35-cycle amplifications, both of the PCR products can be detected when cDNA from whole brain, cortex, cerebellum, and olfactory bulb is used, but not with cDNA from any of the other tissues (J.B., unpublished results).

To examine the cell-specific expression patterns of the mRNAs, we performed *in situ* hybridization of digoxigenin-labeled rOCNC1 and rOCNC2 probes to sections of rat olfactory epithelium. We also used probes recognizing mRNAs encoding G_{olf} (12) and the I7 olfactory receptor (11) to visualize olfactory neurons and to provide controls for nonspecific background hybridization. G_{olf} mRNA is expressed at high levels throughout the neuronal layer (Fig. 3*B*), whereas I7 mRNA, like other olfactory receptor mRNAs (26, 27), is expressed only in a small subset of neurons (Fig. 3*A*). Both rOCNC1 (Fig. 3*C*) and rOCNC2 (Fig. 3*D*) mRNAs are expressed in the olfactory neuronal layer. There is significant heterogeneity in rOCNC2 expression among individual neurons, whereas rOCNC1 is more homogenously expressed.

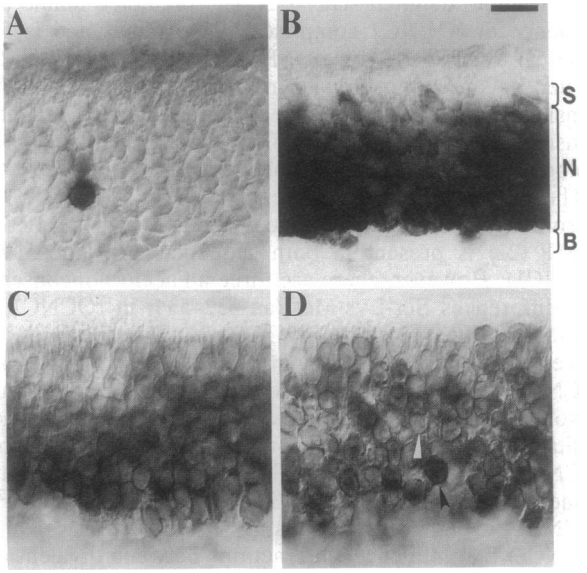

FIG. 3. Expression of rOCNC1 and rOCNC2 mRNAs within the neuronal layer of the olfactory epithelium. We performed *in situ* hybridization to 20-μm horizontal sections of rat olfactory epithelium, using digoxigenin-labeled antisense RNAs as probes. *A–D* are high-magnification photographs (×788), taken with Nomarski optics, of the same region of the epithelium. The olfactory cilia are at the top, and below them are the supporting cell layer (S), the neuronal layers (N), and the basal cell layer (B), as indicated in *B*. Cells expressing a particular mRNA are visualized as dark disks. (*A*) I7 olfactory receptor probe. One I7-expressing neuron is observed in this photograph. The I7 probe, which is about twice as large as the channel probes, also serves as a control for nonspecific hybridization. (*B*) G_{olf} probe. Note the uniform hybridization within the neuronal layers. (*C* and *D*) rOCNC1 and rOCNC2 probes, respectively. Widespread hybridization in the neuronal layers is observed with these two probes. Note the heterogeneity in rOCNC2 mRNA expression. A cell expressing rOCNC2 mRNA at high levels is indicated by a black arrowhead, and a cell lacking the mRNA or expressing it at low levels, by a white arrowhead. *C* and *D* are adjacent sections; *A* and *B* are sections within 50 μM of *C* and *D*. Examination of the epithelial sections at low magnification shows that rOCNC1 and rOCNC2 mRNAs are present in all regions of the epithelium that contain G_{olf} mRNA. (Bar = 5 μM.)

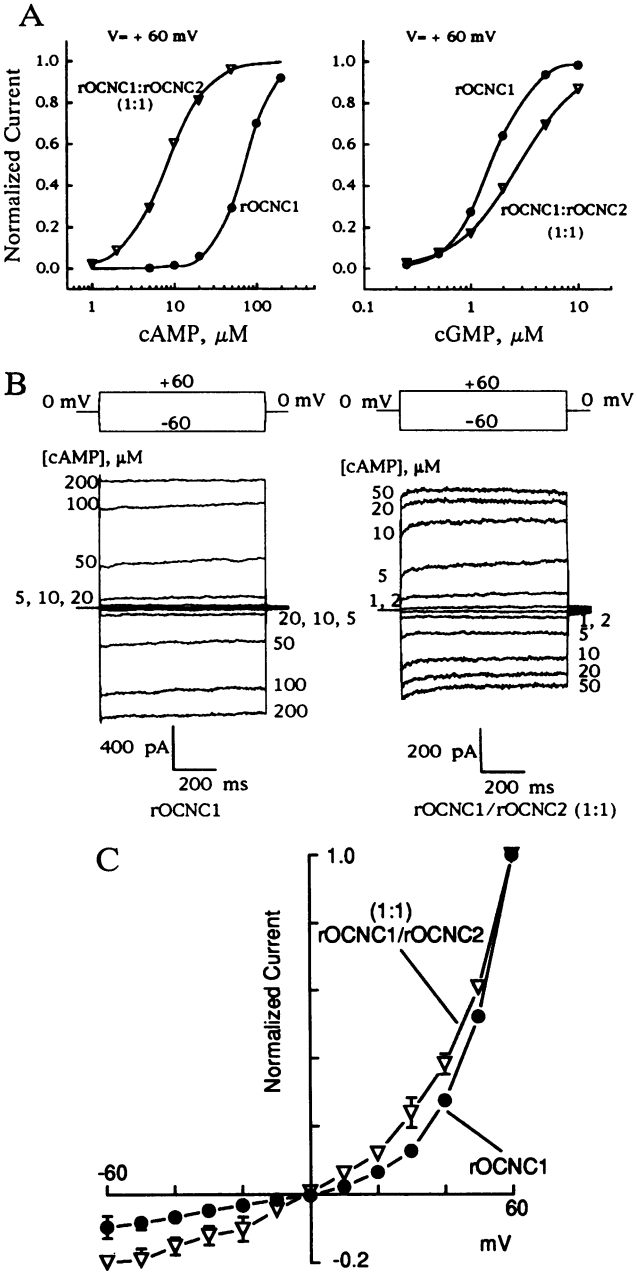

FIG. 4. cng conductances produced by rOCNC1 expression and by rOCNC1/rOCNC2 coexpression. Recordings were obtained from inside-out patches excised from HEK 293 cells transfected with rOCNC1 plasmid or with a 1:1 mixture of rOCNC1 and rOCNC2 plasmids. (*A*) Normalized dose–response relations for cAMP (*Left*) and cGMP (*Right*) at V_m = +60 mV. *Left* is derived from macroscopic current data for the two cells shown in *B*. *Right* displays cGMP results from two other cells. Currents were measured at the end of the 800-ms voltage pulse. The symbols represent the average responses; the smooth lines are described by the Hill equations with best-fitting values. (*B*) Macroscopic currents recorded from two patches (*Left*, rOCNC1; *Right*, rOCNC1/rOCNC2). V_m was stepped from 0 to +60 or −60 mV for 800 ms. The patches were kept in symmetrical divalent cation-free solutions, and the bath contained cAMP at the concentrations indicated. Top traces show the voltage commands for each episode in a trial. Episodes shown are averaged from three to six trials, each taken during a separate series of cAMP applications at ascending concentrations. Leak currents have been subtracted. Filter corner frequency, 2 kHz. (*C*) Current–voltage relation in the presence of extracellular divalent cations. Currents were activated with cAMP at 50 μM for rOCNC1/rOCNC2 patches (n = 3), and at 200 μM for rOCNC1 patches (n = 4). Both were normalized to currents at V_m of +60 mV. Leak currents were subtracted. Error bars indicate SEM.

Table 1. Properties of cyclic nucleotide-activated conductances observed in HEK 293 cells expressing the rOCNC1 and rOCNC1/rOCNC2 channels, compared with those previously measured for the rat native olfactory cng channels (7)

Channel type	V_m, mV	cAMP		cGMP		EC_{50} (cAMP)/ EC_{50} (cGMP)
		EC_{50}, μM	Hill coefficient	EC_{50}, μM	Hill coefficient	
rOCNC1	−60	48 ± 4.6 (n = 11)	2.8 ± 0.3 (n = 11)	1.6 ± 0.2 (n = 7)	2.1 ± 0.2 (n = 7)	30
	+60	47 ± 3.5 (n = 11)	2.6 ± 0.3 (n = 11)	1.4 ± 0.1 (n = 7)	2.4 ± 0.4 (n = 7)	34
rOCNC1/rOCNC2	−60	10.8 ± 1.7 (n = 8)	1.8 ± 0.2 (n = 8)	2.7 ± 0.5 (n = 8)	1.8 ± 0.1 (n = 8)	4.0
	+60	7.3 ± 0.8 (n = 8)	1.9 ± 0.1 (n = 8)	2.9 ± 0.4 (n = 8)	1.6 ± 0.1 (n = 8)	2.5
Native channel	+50	2.5	1.8	1.0	1.3	2.5

Results are given as mean ± SEM.

These patterns suggest that some olfactory neurons may express only the rOCNC1 channel. This could explain earlier observations that the cng conductance of a subpopulation of neurons exhibited a lower sensitivity to cAMP (3). *In situ* hybridization to brain sections shows that both channel subunit mRNAs are also expressed in subsets of neurons in the olfactory bulb, cerebellum, and cortex (J.B., unpublished results).

To determine whether rOCNC2 could function as a cng channel, we transiently transfected HEK 293 cells with an rOCNC2 expression vector. Ten to 40% of the transfected cells exhibited bright surface staining with an rOCNC2-specific antiserum (J.B., unpublished results), but we could not detect any cyclic nucleotide-activated conductances in excised inside-out patches from these cells.

To evaluate whether rOCNC2 could alter the properties of the rOCNC1 channel, we transfected HEK 293 cells with the rOCNC1 expression vector alone or with a mixture of the rOCNC1 and rOCNC2 plasmids at a 1:1 molar ratio. At a membrane potential (V_m) of +60 mV, an inside-out patch from an rOCNC1-expressing cell displayed a cyclic nucleotide-activated conductance with an EC_{50} for cAMP of 64 μM. A cell expressing both subunits, in contrast, had an EC_{50} for cAMP of 6.3 μM at +60 mV (Fig. 4*A Left*; macroscopic current traces from these two patches are shown in Fig. 4*B*). While expression of rOCNC2 increased the apparent affinity of the channel for cAMP, it had the opposite effect for cGMP. The EC_{50} for cGMP was 1.5 μM for a cell expressing only rOCNC1 but was 2.8 μM for a cell expressing both subunits (Fig. 4*A Right*). The data obtained from 34 patches are summarized in Table 1.

Table 1 also shows that the Hill coefficients for the rOCNC1/rOCNC2 channel approximate those observed for the native channel (7) and are significantly lower than for the rOCNC1 channel. We do not know whether the lower Hill coefficients of the rOCNC1/rOCNC2 channel are due to a reduced cooperativity at the molecular level or to the presence of a heterogeneous population of channels in the patch that have different subunit stoichiometries. In cells cotransfected with rOCNC2 and rOCNC1 plasmids at ratios of 3:1 or 6:1, the average EC_{50} for cAMP was 6.9 ± 0.8 at +60 mV (n = 8). Thus, increasing the relative proportion of rOCNC2 does not increase the sensitivity to cAMP beyond the values observed with a 1:1 ratio. The EC_{50} values for both cAMP and cGMP that we measured for the rOCNC1/rOCNC2 channel in HEK 293 cells are ≈3 times those observed for the native rat channel (7) (Table 1). This may be due to differences in experimental conditions, in posttranslational modification, or in interactions with cell-specific modulatory factors. For example, a recent study demonstrated that the cyclic-nucleotide sensitivity of the rOCNC1 and native rat channels can be dramatically altered by direct interaction with Ca^{2+}/calmodulin (28).

The differences in apparent agonist affinity between the heterooligomeric and homooligomeric channels may be partially due to the three adjacent nonconservative amino acid substitutions within the highly conserved CN domain (Fig. 1). In the determined three-dimensional structures of CN domains from another protein (21), these three positions are within a loop that forms part of the cyclic nucleotide-binding pocket.

The rOCNC1/rOCNC2 channel shows outward rectification in symmetrical divalent-free solutions. The kinetic basis for this rectification is a current relaxation (time constant of 30–50 ms) to smaller or larger amplitudes following a step from zero to negative or positive membrane potentials, respectively (Fig. 4*B Right*). The relaxation was not observed for cells transfected with rOCNC1 alone (Fig. 4*B Left*). The increased voltage dependence of the heterooligomeric channel could be due to the larger number of positive charges in the S4 domain of rOCNC2 relative to rOCNC1.

In the presence of extracellular divalent cations, both the homooligomeric and heterooligomeric channels are outwardly rectifying, but the divalents have a smaller effect on the heterooligomeric channel. In the absence of divalent cations, the ratio of current amplitudes at −60 and +60 mV (I^{-60}/I^{+60}) was 0.84 for rOCNC1 (see Fig. 4*B*), and this ratio decreased by 8-fold, to 0.11, with the inclusion of 2 mM Ca^{2+} and 1 mM Mg^{2+} in the extracellular solution (Fig. 4*C*). Divalent cations had a smaller effect on the rOCNC1/rOCNC2 channel, decreasing I^{-60}/I^{+60} by only a factor of 3 (from 0.62 to 0.2). These data suggest that the two channels could have different Ca^{2+} permeabilities. Permeability to Ca^{2+} is likely to be functionally important since a major component of the depolarizing current in olfactory neurons is carried by a Ca^{2+}-activated Cl^- conductance (8–10).

The rOCNC1/rOCNC2 channel also differs from the rOCNC1 channel in its single-channel properties. The open-

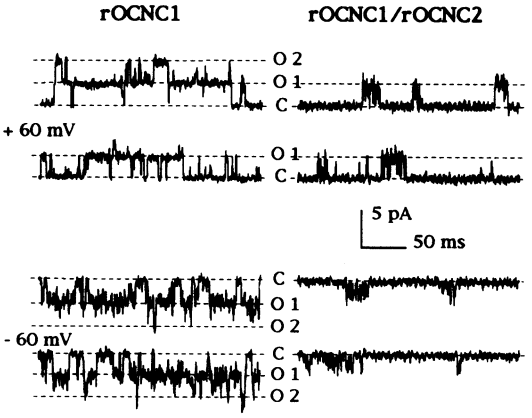

FIG. 5. Single-channel properties of homooligomeric rOCNC1 channel (the patch contained hundreds of channels, thus 0.1 μM cAMP was used) (*Left*) and heterooligomeric rOCNC1/rOCNC2 channel (the patch contained one channel, so 2 μM cAMP was used) (*Right*). V_m was +60 mV (*Upper*) or −60 mV (*Lower*). O1 and O2 represent the conductance from the openings of one and two channels within the rOCNC1 patch, respectively. C represents the closed state. The dotted line represents the current amplitude corresponding to a single-channel conductance of ≈48 pS. Consecutive sweeps are shown.

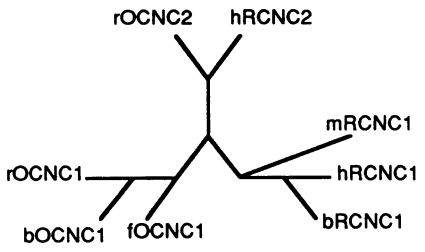

FIG. 6. One unrooted parsimonious tree of cng channel coding-region DNA sequences, calculated on a VAX computer using the Phylogeny Inference Package of programs (30). Prefixes: h, human; r, rat; m, mouse; b, bovine; f, catfish.

ings of the rOCNC1 channel are stable, last for tens of milliseconds, and have a maximal conductance of ≈48 pS at +60 mV (Fig. 5 *Left*). The rOCNC1/rOCNC2 channel is flickery at +60 mV, making it difficult to accurately measure single-channel conductances. At −60 mV, the flickering is further accentuated (Fig. 5 *Right*). This reduces the effective single-channel conductance and contributes to outward rectification. Flickery opening behavior has also been observed for the native channel (7).

DISCUSSION

We have identified a second subunit of the rat olfactory cng channel, rOCNC2. This subunit does not form a functional channel by itself but heterooligomerizes with the previously identified olfactory channel, rOCNC1, to produce a channel whose electrophysiological behavior differs from that of the homooligomeric rOCNC1 channel.

Additional subunits that modulate channel properties have been identified for K^+ channels and for various ligand-gated channels. A modulatory subunit for the human rod cng channel, hRCNC2, has also been described (19). This subunit does not function as an ion channel when expressed alone, but can form functional heterooligomers with the previously characterized rod cng channel, hRCNC1. Compared with the hRCNC1 channel, the hRCNC1/hRCNC2 channel is more similar to the native photoreceptor channel in its sensitivity to drug blockade and in its single-channel properties. The openings of both olfactory and retinal heterooligomeric channels are flickery, while the openings of both homooligomeric channels are stable. Like rOCNC2, hRCNC2 is shorter at its N terminus than the first rod channel subunit.

The data described above indicate that the native cng channels in olfactory neurons and in retinal rods are similar in many respects. An evolutionary tree of the cng channel sequences (Fig. 6) suggests that the rOCNC2 and hRCNC2 subunits arose from a common ancestral protein after the rOCNC1 and hRCNC1 subunits diverged. Thus, the olfactory and retinal channels may have once shared a common modulatory subunit.

The rOCNC2 subunit confers several properties that are characteristic of the native channel from olfactory neurons but differ from those of the homooligomeric rOCNC1 channel. These include agonist sensitivity, rectification, and single-channel behavior. The ratio of the EC_{50} values for cAMP versus cGMP is 34 for the homooligomeric rOCNC1 channel and 2.5 for the heterooligomeric rOCNC1/rOCNC2 channel (Table 1). The value of 2.5 is equal to that observed for the native rat channel from olfactory neurons. Our results, together with the studies on the retinal channel (19), provide molecular and functional evidence for the presence of heterooligomeric cng channels *in vivo*.

Note Added in Proof. Similar data on the rOCNC2 channel subunit have been obtained by E. Liman and L. Buck, and a paper describing their results is in press in *Neuron*.

We thank T.-Y. Chen and K.-W. Yau for helpful discussions, HEK 293 cells, and an rOCNC1 clone; W. Zagotta for providing the sequences of the CN1 and CN2 primers; Genentech for the pCIS plasmid; M. Quick and Y. Uezono of Caltech for experimental contributions to the early phase of this project; and L. Buck and E. Liman for communicating data before publication. J.B. was supported by a National Institutes of Health graduate training grant and an Achievement Award for College Scientists. This work was supported by grants from the National Institute of Mental Health and the National Institutes of Health to K.Z., H.A.L., and N.D.

1. Reed, R. R. (1992) *Neuron* **8**, 205–209.
2. Lancet, D. & Ben-Arie, N. (1993) *Curr. Biol.* **3**, 668–674.
3. Nakamura, T. & Gold, G. H. (1987) *Nature (London)* **325**, 342–344.
4. Kurahashi, T. (1990) *J. Physiol. (London)* **430**, 355–371.
5. Firestein, S., Darrow, B. & Shepherd, G. M. (1991) *Neuron* **6**, 825–835.
6. Zufall, F., Firestein, S. & Shepherd, G. M. (1991) *J. Neurosci.* **11**, 3573–3580.
7. Frings, S., Lynch, J. W. & Lindemann, B. (1992) *J. Gen. Physiol.* **100**, 45–67.
8. Kleene, S. J. (1993) *Neuron* **11**, 123–132.
9. Kurahashi, T. & Yau, K.-W. (1993) *Nature (London)* **363**, 71–74.
10. Lowe, G. & Gold, G. (1993) *Nature (London)* **366**, 283–286.
11. Buck, L. & Axel, R. (1991) *Cell* **65**, 175–187.
12. Jones, D. T. & Reed, R. R. (1989) *Science* **244**, 790–795.
13. Bakalyar, H. A. & Reed, R. R. (1990) *Science* **250**, 1403–1406.
14. Dhallan, R. S., Yau, K.-W., Schrader, K. A. & Reed, R. R. (1990) *Nature (London)* **347**, 184–187.
15. Ludwig, J., Margalit, T., Eismann, E., Lancet, D. & Kaupp, U. B. (1990) *FEBS Lett.* **270**, 24–29.
16. Goulding, E. H., Ngai, J., Kramer, R. H., Colicos, S., Axel, R., Siegelbaum, S. A. & Chess, A. (1992) *Neuron* **8**, 45–58.
17. Saiki, R. K., Gelfand, D. H., Stoffel, S., Scharf, S. J., Higuchi, R., Horn, G. T., Mullis, K. B. & Erlich, H. A. (1988) *Science* **239**, 487–491.
18. Schaeren-Wiemers, N. & Gerfin-Moser, A. (1993) *Histochemistry* **100**, 431–440.
19. Chen, T.-Y., Peng, Y.-W., Dhallan, R. S., Ahamed, B., Reed, R. R. & Yau, K.-W. (1993) *Nature (London)* **362**, 764–767.
20. Kaupp, U. B. (1991) *Trends NeuroSci.* **14**, 150–157.
21. Shabb, J. B. & Corbin, J. D. (1992) *J. Biol. Chem.* **267**, 5723–5726.
22. Altenhofen, W., Ludwig, J., Eismann, E., Kraus, W., Bonigk, W. & Kaupp, U. B. (1991) *Proc. Natl. Acad. Sci. USA* **88**, 9868–9872.
23. Heginbotham, L., Abramson, T. & MacKinnon, R. (1992) *Science* **258**, 1152–1155.
24. Root, M. J. & MacKinnon, R. (1993) *Neuron* **11**, 459–466.
25. Eismann, E., Muller, F., Heinemann, S. H. & Kaupp, U. B. (1994) *Proc. Natl. Acad. Sci. USA* **91**, 1109–1113.
26. Ressler, K. J., Sullivan, S. L. & Buck, L. B. (1993) *Cell* **73**, 597–610.
27. Vassar, R., Ngai, J. & Axel, R. (1993) *Cell* **74**, 309–318.
28. Chen, T.-Y. & Yau, K.-W. (1994) *Nature (London)* **368**, 545–547.
29. Bradley, J., Uezono, Y., Davidson, N., Lester, H. A. & Zinn, K. (1992) *Soc. Neurosci. Abstr.* **18**, 596.
30. Felsenfeld, J. (1989) *Cladistics* **5**, 164–166.